International Journal of Scientific & Engineering Research, Volume 5, Issue 3, March-2015
ISSN 2229-5518


# Optimal Design of High-Speed Interior Permanent-Magnet Synchronous Machine Using Bees Algorithm

Amin Ghaghishpour
Amin_ghaghishpour@yahoo.com

**Abstract—** Permanent magnet synchronous machines become more and more popular due to their reliable construction and very good performance in mechatronics systems. Permanent magnet synchronous motors (PMSM) are one of the most proper and efficient motors in electricity industries, which are good candidates for applications such as naval and space systems, electric vehicles and, etc. This paper presents a multiphysic modeling of an interior permanent-magnet synchronous machine (IPMSM) dedicated to high speed, including magnetic, electric, thermal, and mechanical aspects. The proposed analytical models are verified using finite-element (FE) computations. The bees algorithm is used to optimal design of IPMSM for a high-speed compress or application that develops 30 kW at 20 000 r/min. The simulation results show that the proposed method has high performance.

**Index Terms**— Bees algorithm, IPMSM, high-speed, design, optimal.

## 1 INTRODUCTION

PERMANENT, Magnet Synchronous Motors (PMSMs) have been widely used in many industrial applications. Permanent magnet synchronous motors are developed from conventional synchronous motors. In a conventional synchronous motors, there is multi-phase winding in stator and an excitation winding in rotor, but in PMSMs excitation winding is cancelled and replaced by permanent magnets. This replacement brings noticeable features to these machines. Above all, efficiency of the motor is promoted because of lack of copper loss of excitation winding. Besides, power factor of these motors are high which is a good feature for power system. Drawback of PMSMs is that the materials used for producing permanent magnets are very costly, and they are difficult to work in manufacturing [1].

The hybrid electric vehicle (HEV) permits combining the advantages of thermal and electrical motorization while minimizing their disadvantages [2, 3]. The electrical drives represent actually the common issue in urban transportation. Since the series production of hybrid vehicles has already started, the electrical machines will shortly forestall the automobile market [4]. That is the reason why several researchers have studied different technologies of electrical machines for this kind of application such as asynchronous machine, synchronous machine, switched reluctance machine, switching-flux synchronous machine or axial flux machine [5- 10].

Many research papers have been published in modeling, simulation, investigation and analysis of permanent magnet synchronous motors (PMSM). In Refs. [11,12] for determining the velocity and rotor position of an IPMSM, classical electro-mechanical sensors, tacho-generator for velocity and encoder for rotor position, were applied. In [13,14] for determining the above mentioned parameters for a PMSM the same procedure as [11,12] was applied. In the paper [15] for minimizing troubles and improving the reliability of the control system and also for economical aspects the ordinary sensors were cancelled from the overall system, and velocity as well as rotor position were computed by using machine parameters and measuring voltage and current of the PMSM.

In [16] the extended Kalman filter (EKF) estimator has been used to estimate rotor current and rotor impedance in an induction motor (IM). In paper [17] an extended Kalman filter is used to estimate the inverse rotor time constant on-line by only using measurements of the stator voltages and currents, and rotor speed of an IM.

In papers [18,19] the same method as [8] was applied, but in order to reduce the synchronous motor (SM) modeling and measurement errors, EKF was employed. At the same time, estimation of motor speed and rotor position by EKF was also obtained. But, in [20] the estimated results of speed have not been presented.

The paper is organized as follow. Section two describes the machine model. Section 3 presents the optimization algorithms including bee's algorithm and particle swarm optimization algorithm. Section 4 presents the optimization problem. Section 5 presents the some simulation results and finally section 6 conclude the paper.

## 2 MACHINE MODEL

The IPMSM rotor uses magnets, inserted between the pole pieces. This composition cancels the need of a costly bandage that would make the manufacturing more complex. This is of interest at high speed where the machine should have low flux densities [14]. The number of pole is fixed to 6 and the slot number to 36. Fig. 1 shows the analytical modeling of IPMSM.

- *Amin Ghaghishpour, Department Electrical Engineering Aliabad Branch, Islamic Azad University of Iran, Amin_ghaghishpour@yahoo.com*

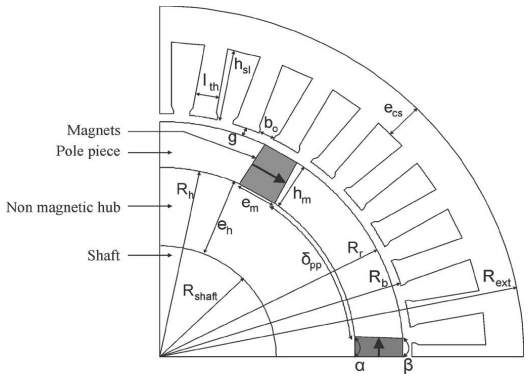


Fig. 1. Geometry of the machine

In this study we apply some approximations for simplicity of machine formulation such as: The magnets considered in rectangular shape, the pole fixations are cancelled, the hub is considered completely smooth, also the shaft of machine, and its air gap is considered to have constant value. Ref [21] describe the computation principle of the $dq$. The base of calculation is magnetic flux through the winding. More details regarding the steps for determining the parameters' expressions of the $dq$ linear model can be found in [21].

High-speed rotation modifies the classical loss balance between iron and copper losses. Copper loss is the term often given to heat produced by electrical currents in the conductors of transformer windings, or other electrical devices. Copper losses are an undesirable transfer of energy, as are core losses, which result from induced currents in adjacent components. The term is applied regardless of whether the windings are made of copper or another conductor, such as aluminium. Hence the term winding loss is often preferred. The term load loss is closely related but not identical, since an unloaded transformer will have some winding loss.

There are also electromagnetic losses in the rotor due to time and space harmonics occurring in the pole pieces and in the magnets. Electric motors do not transfer 100% of the input electrical energy into kinetic mechanical energy. A certain percentage of electrical energy is "lost" during the conversion to mechanical energy. These losses, which are manifested as electrical power losses (waste heat due to the electrical resistance of the windings, conductor bars and end rings), magnetic core losses, stray load losses, mechanical losses, and brush contact losses, reduce what is known as the "energy efficiency" of motors. The electrical power losses account for more than half of a motor's total losses. In order to use the copper winding at best, the wire diameter must be chosen small enough to prevent penetration and proximity effects from being too important.

Eq. (1) presents the the phase resistance expression:

$$R_{ph} = \rho_{Cu} L_{turn} \frac{N_s N_{cond/slot}}{N_{par} k_{fill} S_{slot}} \quad (1)$$

In this equation, $k_{fill}$ is filling factor and is set to 0.55. Eq. (2) shows copper loss:

$$P_{Cu} = 3R_{ph}\left(\frac{I_{ph}}{\sqrt{2}}\right)^2 \quad (2)$$

High speed machine involves high electrical frequency and this high speed is the cause of more iron loss. For this purpose we determine the number of pole at low number and the iron thin is between o.2- 0.35 millimeter. The iron losses are also referred to as "core losses" and represent all the magnetic losses in the motor due to the varying flux in the motor's magnetic material. These losses can be classified in two types: 1) Hysteresis losses, 2)Eddy current losses. If we have linear machine situation, the air gap magnetic flux density, $B_{ag}$ , is computed as the sum of the magnetic flux density due to magnets, $B_f$ , and the magnetic flux densities due to d-axis, $B_d$ , and q-axis, $B_q$ , stator armature current reaction, as detailed in [21]. Fig. 2 illustrates this fact. Also table 1 shows iron loss formulation parameters for M330-35 materials.

$$B_{th}(\theta) = \frac{k_{ds}}{k_{stack}} \int_{\theta-(\tau_s/2)}^{\theta+(\tau_s/2)} B_{ag}(u)\,du \quad (3)$$

$$B_{bi}(\theta) = \frac{1}{k_{stack} e_{bi}} \int_{\theta}^{\theta+\pi} B_{ag}(u) R_b\,du \quad (4)$$

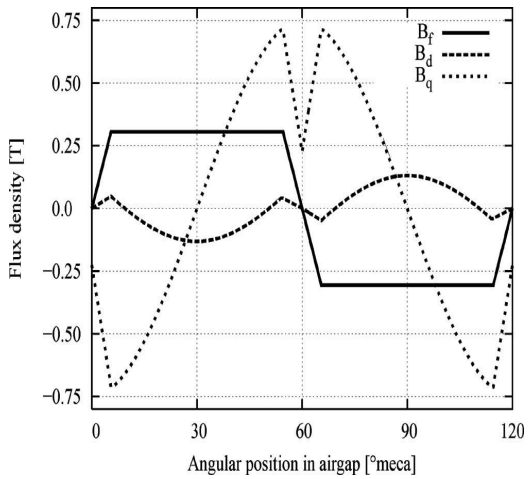


Fig. 2. Example of wave forms of the three components of the air gap magnetic flux density

TABLE 1
IRON LOSS FORMULATION PARAMETERS FOR M330-35 MATERIALS

| Coefficient | Value |
|---|---|
| $\alpha_{ir}$ | 2 |
| $k_H$ | 0.0220 |
| $k_{EC}$ | 0.3873 |
| $k_{EXC}$ | 0 |
| $\gamma$ | 6.04e-4 |

Friction and windage losses (the latter one is also referred to as ventilation loss) are due to all sources of friction and air movement in the motor and may be appreciable in large high speed or
totally enclosed fan cooled motors. Friction losses and windage losses are (unlike the previous components) mechanical losses, and they manifest themselves as a loss of torque (for rotational motors) or force (for linear motors). The air gap friction losses formulation is [22]

$$P_{fric,ag} = C_t \rho_{air} \frac{V_p^3}{2} S_{rot} \qquad (5)$$

Where $C_t$ is a coefficient.

## 3. OPTIMIZATION ALGORITHMS

### 3.1. Bee's Algorithm

Bees Algorithm is an optimization algorithm inspired by the natural foraging behavior of honey bees to find the optimal solution. Fig. 3 shows the pseudo code for the algorithm in its simplest form. The algorithm requires a number of parameters to be set, namely: number of scout bees (n), number of sites selected out of n visited sites (m), number of best sites out of m selected sites (e), number of bees recruited for best e sites (nep), number of bees recruited for the other (m-e) selected sites (nsp), initial size of patches (ngh) which includes site and its neighborhood and stopping criterion. The algorithm starts with the n scout bees being placed randomly in the search space. The fitnesses of the sites visited by the scout bees are evaluated in step 2.

In step 4, bees that have the highest fitnesses are chosen as "selected bees" and sites visited by them are chosen for neighborhood search. Then, in steps 5 and 6, the algorithm conducts searches in the neighborhood of the selected sites, assigning more bees to search near to the best e sites. The bees can be chosen directly according to the fitnesses associated with the sites they are visiting. Alternatively, the fitness values are used to determine the probability of the bees being selected. Searches in the neighborhood of the best e sites which represent more promising solutions are made more detailed by recruiting more bees to follow them than the other selected bees. Together with scouting, this differential recruitment is a key operation of the Bees Algorithm.

However, in step 6, for each patch only the bee with the highest fitness will be selected to form the next bee population. In nature, there is no such a restriction. This restriction is introduced here to reduce the number of points to be explored. In step 7, the remaining bees in the population are assigned randomly around the search space scouting for new potential solutions. These steps are repeated until a stopping criterion is met. At the end of each iteration, the colony will have two parts to its new population representatives from each selected patch and other scout bees assigned to conduct random searches [23].

1. Initialise the solution population.
2. Evaluate the fitness of the population.
3. While (stopping criterion is not met)
//Forming new population.
4. Select sites for neighbourhood search.
5. Recruit bees for selected sites (more bees for the best e sites) and evaluate fitnesses.
6. Select the fittest bee from each site.
7. Assign remaining bees to search randomly and evaluate their fitnesses.
8. End While

Fig. 3. Pseudo code

### 3.2. particle swarm optimization

The basic operational principle of the particle swarm is reminiscent of the behavior of a group, for example, a flock of birds or school of fish, or the social behavior of a group of people . Each individual flies in the search space with a velocity which is dynamically adjusted according to its own flying experience and its companions' flying experience, instead of using evolutionary operators to manipulate the individuals like in other evolutionary computational algorithms. Each individual is considered as a volume-less particle (a point) in the N-dimensional search space. At time step t,the ith particle is represented as: $X_i(t) = (x_{i1}(t), x_{i2}(t), ...., x_{iN}(t))$.The set of positions of m particles in a multidimensional space is identified as $X = \{X_1, ...., X_j, ...., X_l, ...., X_m\}$.The best previous position (the position giving the best fitness value) of the ith particle is recorded and represented as $P_i(t) = (p_{i1}, p_{i2}, ....., p_{iN})$. The index of the best particle among all the particles in the population (global model) is represented by the symbol g. The index of the best particle among all the particles in a defined topological neighborhood (local model) is represented by the index subscript $l$. The rate of movement of the position (velocity) for particle $i$ at the time step $t$ is represented

as $V_i(t) = (v_{i1}(t), v_{i2}(t), ...., v_{iN}(t))$ .The particle variables are manipulated according to the following equation (global model [24]):

$$v_{in}(t) = w_i * v_{in}(t-1) + c_1 * rand1(.) * (p_{in} - x_{in}(t-1)) + c_2 * rand2(.) * (p_{gn} - x_{in}(t-1)) \quad (6)$$

$$x_{in}(t) = x_{in}(t-1) + v_{in}(t)$$

where n is the dimension . $(1 \le n \le N)$, $c_1$ And c2 are positive constants, rand1 (.) and rand2 (.) are two random functions in the range [0, 1], and $w$ is the inertia weight. For the neighborhood $(lbest)$ model, the only change is to substitute $p_{\ln}$ for $p_{gn}$ in the equation for velocity. This equation in the global model is used to calculate a particle's new velocity according to its previous velocity and the distance of its current position from its own best experience $(pbest)$ and the group's best experience $(gbest)$. The local model calculation is identical, except that the neighborhood's best experience is used instead of the group's best experience. Particle swarm optimization has been used for approaches that can be used across a wide range of applications, as well as for specific applications focused on a specific requirement. Its attractiveness over many other optimization algorithms relies in its relative simplicity because only a few parameters need to be adjusted.

## 4. OPTIMIZATION PROBLEM

The researcher is considering investigating the design problem into an optimization problem constrained by limits over the research space and the solution space. For the targeted application, the machine can be designed for only one operating point and it must develop 30 kW at 20 000 r/min. In this paper a double objective optimization of efficiency (η) and machine weight (M) is investigated. The objective functions are presented as follows:

$$\eta = \frac{P_{mech}}{P_{mech} + P_{ir} + P_{Cu} + P_{fric}} \quad (6)$$

$$M = M_{pole\_piece} + M_{teeth} + M_{copper} + M_{back\_iron} + M_{magnet} + M_{hub} + M_{shaft} \quad (7)$$

$$\text{Fitness} = \eta + \frac{1}{M} \quad (8)$$

In this optimization problem, we have 13 optimization parameters. These optimization problems are as follow:

1 stator outer diameter
2 slot depth
3 Slot width
4 air gap length
5 stator bore diameter
6 magnet height and width
7 magnet width
8 hub radius
9 stack length
10 magnet
11 current density
12 number of turns connected in series
13 load angle

Table 2 shows some bounds of optimization variables. This optimization will satisfy the limits expressed in Table 3.

TABLE 2
OPTIMIZATION VARIABLES RANGE

| Quantity | Definition range |
|---|---|
| External radius [mm] | [50 - 100] |
| Stack length [mm] | [50 - 250] |
| Air gap [mm] | [0.5 - 10] |
| Magnet width [mm] | [0.5 - 10] |
| Current density | [1 - 25] |
| Conductor per slot | [2 - 20] |
| Magnet remanence | [0.8 - 1.3] |
| Load angle | [0 - 90] |
| DC bus voltage [V] | 500 |

TABLE 3
OPTIMIZATION CONSTRAINT

| Quantity | Value |
|---|---|
| Power | 30 kw |
| Speed | 20.000 rpm |
| Ambient temperature | $40^{\circ}$ |
| Supply constraint | $V_{ph} < V_{DC}/2$ |
| Copper temperature | $T_{eu} < 130^{\circ}$ |
| Mechanical constraint | <300 MPa |
| Maximum flux density | <1.4 T |
| Static deformation | $\frac{g}{10} > f_d$ |
| First critical speed | $\Omega_{cl} > 1.25\Omega$ |
| Demagnetization field | $> H_{cj}$ |

## 5 SIMULATION RESULTS

The result of optimization method is represented in this section. Table 4 shows the machine constants and parameters. The tables 5 and 6 show the bee's algorithm and PSO parameters.

TABLE 4
MACHINE CONSTANTS AND PARAMETERS

| | |
|---|---|
| $b_0$ | Stator slot opening. |
| $B$ | Iron path magnetic flux density |
| $\hat{B}$ | Iron path magnetic flux density magnitude. |
| $B_{ag}$ | Air gap magnetic flux density |
| $B_{bi}$ | Stator back iron magnetic flux density |
| $B_d$ | Air gap magnetic flux density due to *d*-axis stator current reaction |
| $B_f$ | Air gap magnetic flux density due to magnets. |
| $B_k$ | Amplitude of the *k*th term of *B* Fourier series decomposition |
| $B_q$ | Air gap magnetic flux density due to *d*-axis stator current reaction |
| $B_r$ | Magnet remanence |
| $B_{th}$ | Stator tooth magnetic flux density |
| $C_t, C_r$ | Windage coefficients |
| $E_Y$ | Young's modulus. |
| $e_{ag}$ | Constant air gap corrected with Carter's coefficient |
| $e_{bi}$ | Stator back iron thickness |
| $e_h$ | Hub thickness |
| $e_m$ | Magnet width |
| $F$ | Pole piece centrifugal effort |
| $f$ | Electrical frequency |
| $f_d$ | Rotor maximum bend distance |
| $g$ | Air gap |
| $g_0$ | Gravitational acceleration |
| $h_m$ | Magnet height. |
| $h_{sl}$ | Slot depth |
| $H_{cj}$ | Coercive force |
| $I_d, I_q$ | Stator electromagnetic current amplitudes |
| $I_{ph}, I_{ph,d}, I_{ph}$ | Stator terminal current amplitude and its components in dq frame |
| $I_{ir,d}, I_{ir,q}$ | Current amplitudes corresponding to iron loss |
| $k_C$ | Carter's coefficient |
| $k_{ds}$ | Tooth concentration factor between tooth and air gap |
| $k_w$ | Global winding coefficient for first harmonic |
| $k_{fill}$ | Slot filling factor |
| $k_{stack}$ | Lamination stacking factor |
| $L_{act}$ | Active stack length. |

TABLE 5
PARAMETERS OF BA

| | |
|---|---|
| Number of scout bees, *n* | 20 |
| Number of sites selected for neighborhood search, *m* | 8 |
| Number of best "elite" sites out of *m* selected sites, *e* | 4 |
| Number of bees recruited for best *e* sites, *nep* | 4 |
| Number of bees recruited for the other (*m*-*e*) selected sites, *nsp* | 4 |
| Number of iterations, *R* | 100 |

TABLE 6
COEFFICIENT VALUES IN THE PSO ALGORITHM

| | |
|---|---|
| Number of particles | 10 |
| Error limit | 0.001 |
| Acceleration constant | 3 |
| Maximum velocity | 8 |
| Maximum number of iterations | 100 |
| Size of the local neighborhood | 2 |
| Constants $c_1 = c_2$ | 2.1 |

### 5.1. Bees algorithm and PSO performance

The obtained results by bees algorithm is presented in this section. In the solved solution we have 97.10% efficiency and 17.43 kg weight. Table 7 shows the characteristics of machine. Also, FE verification is made in non linear conditions. At the rated working point, the iron losses are at 443 watt, the copper losses at 437 watt, and the windage losses at 28.4 watt. As mentioned before, copper losses are much more important than iron losses. In the obtained results, balance between iron and copper losses is achieved. The copper temperature is computed at $98^{\circ}C$, the dovetail constraint at 283 MPa, the hub constraint at 120 MPa. Also table 8 shows the obtained results using PSO. It can be seen that the performance of BA is better than PSO.

TABLE 7
BEST BEE OR OPTIMAL PARAMETER FOR MACHINE

| | |
|---|---|
| Power | 30 |
| Speed | 20.000 |
| External radius [mm] | 77.11 |
| Stack length [mm] | 135.92 |
| Inner stator radius [mm] | 45.65 |
| Hub radius [mm] | 28.7 |
| Shaft radius [mm] | 10.6 |
| Tooth height [mm] | 16.7 |
| Tooth width [mm] | 3.6 |
| Air gap [mm] | 6.2 |
| Magnet height [mm] | 10.6 |
| Magnet width [mm] | 10 |
| Turn number | 12 |
| Current [A] | 197.94 |
| Line to line voltage [V] | 188.9 |
| Remanence induction [T] | 1.3 |
| Load angle | 11.7 |

TABLE 8
BEST PARTICLE OR OPTIMAL PARAMETER FOR MACHINE

| | |
|---|---|
| Power | 30 |
| Speed | 20.000 |
| External radius [mm] | 77.03 |
| Stack length [mm] | 135.6 |
| Inner stator radius [mm] | 45.3 |
| Hub radius [mm] | 28.1 |
| Shaft radius [mm] | 10.9 |
| Tooth height [mm] | 16.4 |
| Tooth width [mm] | 3.5 |
| Air gap [mm] | 6.1 |
| Magnet height [mm] | 10.9 |
| Magnet width [mm] | 10 |
| Turn number | 12 |
| Current [A] | 197.66 |
| Line to line voltage [V] | 188.2 |
| Remanence induction [T] | 1.23 |
| Load angle | 11.44 |
| Efficiency | 96.55% |
| Weight | 17.67 kg |

5.2. Performance evaluation with optimization in different runs

In this sub-section, for evaluating the performance of the BA, three different runs have been performed. Fig. 6 shows a typical increase of the fitness of the best individual fitness of the population obtained from proposed system for different runs. As indicated in this figure, its fitness curves gradually improved from iteration 0 to 100, and exhibited no significant improvements after iteration 40 for the five different runs. The optimal stopping iteration to get the highest performance for the five different runs was around iteration 30–40.

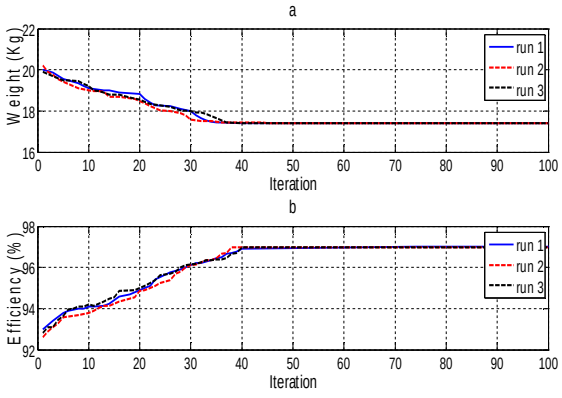


Fig. 6. Evolution of BA for different runs

5.3. Comparison with other optimization algorithms

In order to compare the performance of bees algorithm with another nature inspired algorithms, we have used several nature inspired algorithms such as genetic algorithm (GA) [25], imperialist competitive algorithm (ICA) [26] to solve the optimization problem. Table 9 shows the obtained results. It can be seen that the success rates of bee's algorithm is higher than the performance of other systems.

TABLE 9
COMPARISON AMONG THE PERFORMANCE OF GA, ICA AND PSO

| Optimizer | Efficiency | Weight (kg) |
|---|---|---|
| GA | 96.53% | 17.6 |
| ICA | 95.98& | 17.55 |
| BA | 97.0% | 17.40 |

## 6 CONCLUSION

In this paper a multiphysic modeling of an IPMSM is presented and optimized. In the proposed method the several aspects of machine such as magnetic aspect, thermal aspect, electrical aspect, and mechanical aspect are investigated. An objective function has been proposed covering the power losses, material cost and volume of the motor besides the mechanical and electrical requirements. This method is based on capability of population-based optimization algorithms in finding the optimal solution. One sample case is used to illustrate the performance of the design approach and optimization technique. The superior performance of the BA is due to its ability to simultaneously refine a local search, while still searching globally. Also, simulation results illustrate that BA have a little dependency on variation of the parameters. In addition, BA was very fast, requiring a few seconds to find the optimum.

## REFERENCES

[1] Reza Ilka. Design Optimization for Total Volume Reduction of Permanent Magnet Synchronous Generators. International Journal of Smart Electrical Engineering, Vol.2, No.3, Summer 2013. p.143:149

[2] C.C. Chan, A. Bouscayrol, K. Chen, Electric, hybrid, and fuel-cell vehicles: architectures and modeling, IEEE Transactions on Vehicular Technology 59 (2) (2010) 589–598.

[3] A. Chebak, P. Viargoure, J. Cros, Optimal design of a high-speed slotless permanent magnet synchronous generator with soft magnetic composite stator yoke and rectifier load, Mathematics and Computers in Simulation 81 (2) (2010) 239–251.

[4] O. De La Barière, H. Ben Hamed, M. Gabsi, Axial flux machine design for hybrid traction applications, in: IET Proceedings of the Power Electronics, Machines and Drives Conference, York, UK, April 2–4, 2008.

[5] D. Fodorean, S. Giurgea, A. Djerdir, A. Miraoui, Numerical approach for optimum electromagnetic parameters of electrical machines used in vehicle traction applications, Energy Conversion and Management 50 (5) (2009) 1288–1294.

[6] Z.Q. Zhu, C.C. Chan, Electrical machines topologies and technologies on electric, hybrid, and fuel cell vehicles, in: IEEE

Proceedings of the Vehicle Power and Propulsion Conference, Hei Longjiang, China, September 3–5, 2008.

[7] Z.Q. Zhu, Fractional slot permanent magnet brushless machines and drives for electric and hybrid propulsion systems, in: Proceedings of Ecologic Vehicles and Renewable Energies (EVER), Monaco, March 26–29, 2009.

[8] Z.Q. Zhu, Y.S. Chen, D. Howe, Iron loss in permanent-magnet brushless AC machines under maximum torque per ampere and flux weakening control, IEEE Transactions on Magnetics 38 (5) (2002) 3285–3287.

[9] P.H. Nguyen, E. Hoang, M. Gabsi, M. Lecrivain, A new method to find the fractional slot windings structures from a distributed slot windings permanent magnet synchronous machine and comparative study for a HEV application, in: IEEE Proceedings of the International Conference on Industrial Technology, Valparaiso, Chile, March 14–17, 2010.

[10] P.H. Nguyen, E. Hoang, M. Gabsi, L. Kobylanski, D. Comdamin, Permanent magnet synchronous machines: performances during driving cycles for a hybrid electric vehicle application, in: IEEE Proceedings of the International Symposium on Industrial Electronics, Bari, Italy, July 4–7, 2010.

[11] T.M. Jahns, G.B. Kliman, T.W. Neumann, Interior permanent-magnet synchronous motors for adjustable-speed drives, IEEE Trans. Ind. Appl. 22 (4) (1986) 738±747.

[12] G. Henneberger, Dynamic behavior and current control methods of brushless DC motors with different rotor designs, in: Proceedings of the European Conference on Power Electronics and Applications, Aachen, Germany, 1989, pp. 289±293.

[13] P. Pillay, R. Krishnan, Modeling, simulation and analysis of permanent-magnet motor drives. Part I: the permanent-magnet synchronous motor drive, IEEE Trans. Ind. Appl. 25 (2) (1989) 265±273.

[14] P. Pillay, R. Krishnan, Control characteristics and speed controller design for a high performance permanent-magnet synchronous motor drive, IEEE Trans. Power Electron. 5 (2) (1990) 151± 159.

[15] H. Watanable, T. Isii, T. Fujii, Dc-Brushless servo system without rotor position and speed sensor, in: Proceedings of the International Conference on Industrial Electronics, Control, and Instrumentation, Cambridge, Massachusetts, 1987, pp. 228±234.

[16] L.C. Zai, T.A. Lipo, An extended kalman ®lter approach to the rotor time constant measurement in PWM induction motor drives, in: Proceedings of the IEEE Industrial Applications Society Annual Meeting, 1987, pp. 177±182.

[17] P.K. Sattler, K. Starker, Control of an inverter ed synchronous machine by estimated pole position, in: Proceeding of the 19th Annual Power Electronics Specialists Conference, Kyoto, 1988, pp. 415± 422.

[18] U. Kirberg, Ph. K. Sattler, State estimation on an inverter fed synchronous motor, in: Proceedings of the European Conference on Power Electronics and Applications, Brussels, 1986, pp. 3.229±3.234.

[19] D.J. Atkinson, P.P. Acarnley, J.W. Finch, Observers for induction motor state and parameter estimation, IEEE Trans. Ind. Appl. 27 (6) (1991) 1119±1127.

[20] H. Madadi Kojabadi. Simulation and analysis of the interior permanent magnet synchronous motor as a brushless AC-drive. Simulation Practice and Theory 7 (2000) 691±707

[21] X. Jannot, J.-C. Vannier, J. Saint-Michel, M. Gabsi, C. Marchand, and D. Sadarnac, "An analytical model for ipm synchronous machine with circumferential magnetization design," presented at 8th Int. Symp. Advanced Electromech. Motion Syst. Electric Drives Joint Symp. Electromotion, Lille, France, 2009.

[22] J. Saari, "Thermal analysis of high-speed induction machines," Acta Polytechnica Scandinavia, Electrical Engineering Series no. 90, Dissertation of Helsinki University of Technology, Espoo, Finland, 1998.

[23] D.T. Pham, A. Ghanbarzadeh, E. Koc¸ , S. Otri, S. Rahim, M. Zaidi, The bees algorithm–a novel tool for complex optimisation problems, in: Intelligent Production Machines and Systems (2006) 454–459.

[24] J. Kennedy, R. Eberhart, Particle swarm optimization, in: Proceedings of IEEE International Conference on Neural Networks 4 (1995) 1942–1948.

[25] K.S. Tang, K.F. Man, S. Kwong, Q. He, Genetic algorithms and their applications, IEEE Signal Processing Magazine 13 (1996) 22–37.

[26] E. Atashpaz-Gargari, C. Lucas. Imperialist competitive algorithm: an algorithm for optimization inspired by imperialistic competition. In: Proceedings of the IEEE Congress on Evolutionary Computation, Singapore (2007) 4661–4667